ISSN: 0067-2904

Novel Fusion Approaches for Enhanced Image Processing with Smoothed Images

Ahmed Asaad Zaeen[1*], Nawras Badeaa Mohammed[2], Haidar J. Mohamad[2], Heba Kh. Abbas[3], Anwar. H. Al-Saleh[4], and Ali A. Al-Zuky[2]

[1]*Remote Sensing Unit, College of Science, University of Baghdad, Iraq*
[2] *Ministry of Science and Technology, Iraq*
[3]*Department of Physics, College of Science for Women, University of Baghdad, Iraq*
[4]*Department of Computer Sciences, College of Science, Mustansiriyah University, Iraq*

Received: 24/10/2023 Accepted: 14/7/2024 Published: 30/3/2025

Abstract

Image fusion is integrating multiple images from many sources and changing them into a single image with clearer and more accurate information. Image fusion techniques have been proposed to enhance distorted input images using a smooth filter to improve the clarity of distorted images. This work fused images resulting from smooth filters (half left and half right) with size windows of (3×3), (5×5), (7×7), (9×9), and (11×11) pixels. The image resulting from the smooth filter towards the right was combined with the image from the smooth filter towards the left using traditional techniques such as addition, multiplication, and new suggested techniques, namely absolute real standard deviation, binary standard deviation, real covariance, and binary covariance. The data examined by quality assessment methods with reference depend on Mutual Information, Correlation Coefficient, Structural Similarity Index metric, Structural Content, Normalized Cross Correlation, and without references like Blind Reference less Image Spatial Quality Evaluator, Naturalness Image Quality Evaluator, Perception-based Image Quality Evaluator, and Entropy. Lena's image shows a different behavior than the cameraman and the personal images because Lena's image has more details, resolution, and sharper contrasts. The best combination method was binary standard division.

Keywords: Smooth filter, mathematical fusion, real and binary standard deviation, real and binary covariance

أساليب دمج مبتكرة لمعالجة الصور المحسنة باستخدام الصور المنعّمة

أحمد أسعد زعين[1*]، نورس بديع محمد [2]، حيدر جواد محمد[2]، هبة خضير عباس[3]، أنوار حسن الصالح[4]، علي عبد داوود[2]

[1]وحدة الاستشعار عن بعد، كلية العلوم، جامعة بغداد، بغداد، العراق

[2] وزارة العلوم والتكنولوجيا، بغداد، العراق

[3] قسم الفيزياء، كلية العلوم للبنات، جامعة بغداد، بغداد، العراق

[4] قسم الحاسوب، كلية العلوم، الجامعة المستنصرية، بغداد، العراق

*Email: ahmed.asaad@sc.uobaghdad.edu.iq

الخلاصة:

دمج الصور هو أسلوب دمج صور متعددة من العديد من المصادر المختلفة وتغييرها إلى صورة واحدة تحتوي على معلومات أكثر وضوحًا ودقة. دمجت الصور الناتجة عن مرشح التنعيم (نصف اليسار ونصف اليمين) مع نوافذ بحجم (3×3)، (5×5)، (7×7)، (9×9)، و(11×11) بكسل. تم اقتراح تقنيات دمج الصور لتحسين الصور المدخلة المشوهة باستخدام مرشح تنعيم لتحسين وضوح الصور المشوهة. دمجت الصورة الناتجة من المرشح التنعيم باتجاه اليمين مع الصورة الناتجة من المرشح التنعيم باتجاه اليسار باستخدام التقنيات التقليدية مثل الجمع والضرب والتقنيات الجديدة المقترحة وهي الانحراف المعياري الحقيقي المطلق، والانحراف المعياري الثنائي، والتغاير الحقيقي، والثنائي التغاير. البيانات التي يتم فحصها بواسطة طرق مثل تقييم الجودة مع المرجع والتي تعتمد على المعلومات المتبادلة، ومعامل الارتباط، ومقياس مؤشر التشابه الهيكلي، والمحتوى الهيكلي، والارتباط المتبادل المعياري، وبدون مرجع مثل مقيم جودة الصورة المكانية، مقيم جودة الصورة الطبيعية، القائم على الإدراك مقيم جودة الصورة والانتروبيا. تظهر صورة لينا سلوكًا مختلفًا عن صورة المصور والصورة الشخصية لأن صورة لينا تحتوي على تفاصيل، ودقة، وتباين أكثر وضوحًا. أفضل طريقة للدمج كانت هي الانحراف المعياري الثنائي.

1. Introduction

Image fusion is a technique that combines the corresponding features of a set of original pictures into a single composite image while preserving all of the essential characteristics of the original images that were used [1]. Analytical and visual image quality can be enhanced by combining multiple images. A compelling image combination can preserve essential data by extracting every important detail from the input images without introducing differences in the fused image [2]. The resulting image shows improved suitability for both mechanical and human discernment. The process of image fusion involves the integration of data obtained from multiple sensors to create a more comprehensive dataset [3]. Recently, several fusion methods have been introduced, such as multi-scale decomposition and sparse representation, to enhance the efficiency of image fusion. The fusion technique is required for a wide range of applications. Many studies have been introduced within this field. Heba K. Abbas *et al*. (2021) proposed algorithms that depended on calculating the standard deviation for each color band for multi-focused images. The evaluation depended on the contrast measure at image edge points and the correlation measure for homogeneous regions. Both methods provided excellent results for the merged image. However, it was better to use entropy for lightness, the Naturalness Image Quality Evaluator, and gradient in the edge regions as a criterion [4].

Dongy Rao *et al*. (2022) proposed an algorithm that used a fusion method based on the iterative joint bilateral filter to fuse the base layer components; a convolutional neural network and local similarity of images were used to fuse the components of the detailed layer. They used a multimodal medical image with structure preservation. The contrast experiments displayed that their algorithm had better fusion results than the state-of-the-art medical image fusion algorithms. However, the speed of the proposed algorithm was not ideal [5]. Xin Jin *et al*. (2023) suggested that the transformer and CNN should be used together for multi-focus image fusion because the transformer was very good at getting the more comprehensive dependencies of image features, and CNN was very good at providing detailed information extraction. The experiment showed that the suggested method of fusion worked better. The problem was that the amount of data they used to train the algorithm was insufficient. Therefore, more training data would make the algorithm better [6].

This study seeks to improve the clarity of distorted images at the grey level (Lena, cameraman, personal) by utilizing image fusion techniques after distorting the input images using the smooth filter for half the left and half the right of the image. Traditional techniques, such as addition, multiplicative, and statistical merging, are employed based on weights (real standard deviation, binary standard deviation, real covariance, and binary covariance). The

quality of the resulting images is evaluated using statistical criteria divided into two groups, dependent on the reference (Mutual Information, Correlation Coefficient, Structural Similarity Index metric, Structural Content, Normalized Cross Correlation), and without reference (Blind Reference Less Image Spatial Quality Evaluator, Naturalness Image Quality Evaluator, Perception-based Image Quality Evaluator, Entropy).

2. Theory and Methods

To improve the clarity of distorted images, researchers have proposed image fusion techniques that involve distorting the input images using a smooth filter using window (3×3), (5×5), (7×7), (9×9), and (11×11) pixels [7]. The mean filter is one of the most straightforward linear filters that computes a weighted sum of the pixel grey levels in a neighborhood and replaces the center pixel with that grey level. If we have an image and its dimensions are N×N, then the procedure used to obtain a smooth image g(x,y) at each point (x, y) is to find the average of the elements of the image in the vicinity of (x, y) using a sliding window using the following relationship [8].

$$g\ (x,y) = \frac{1}{n}\sum_{(i,j)} f(i,j) \quad (1)$$

Where *x* and *y* =0,1, 2,..., N-1, *g* is the output image, and *n* is the number of points using the moving average.

In this work, enhancing the clarity of smoothed images depends on traditional mathematical techniques such as addition and multiplication or statistical merging techniques based on weights (standard deviation and covariance) [9]. The quality of the fused images was evaluated using statistical criteria with and without the reference[10].

$$\sigma_{I_{A,I_B}}(i,j) = \sqrt{\sum_{i=1}^{m}\sum_{j=1}^{n}(I(i,j)-\mu)^2} \quad (2)$$

$$P1 = \frac{\sigma I_A(i,j)}{\sigma I_A(i,j)+\sigma I_B(i,j)} \quad (3)$$

$$P2 = (1-P1) \quad (4)$$

Where *m* and *n* are the number of rows and columns of the merged image, respectively, I (i, j) is a combined image, and μ indicates the mean. $\sigma I_A, \sigma I_B$ are standard deviations for reference images. P1 and P2 are weighed factor.

The proposed integration technique was based on the statistical standard direct covariance (CV) image fusion. Covariance is a method used to determine the number of two random variables that change together. Covariance has a positive number. Therefore, the linear relationship between the variables *x* and *y* is given as[11]:

$$CV_{I_{A,I_B}}(i,j) = \frac{1}{i\times j}\sum_{i=1}^{m}\sum_{j=1}^{n}[\![(I_A(i,j)]\!] - \bar{I}_A\big)\big(I_B(i,j) - \bar{I}_B\big) \quad (5)$$

Where *i* and *j* represent the number of rows and columns, *m* and *n* are the total values for row and column, I_A and I_B are the input image, $\bar{I}\_A$ and $\bar{I}\_B$ are the mean of the input image.

2.1 Quantitative Analysis Criteria

Quantitative analysis is based on mathematical modeling and evaluates the similarity in spectral and spatial characteristics between the merged image (C) and the input images (A and B) using a set of predetermined quality criteria. This work used two approaches for quantitative analysis, one involving a reference image and the other without. The evaluation of the merged image's performance involved the utilization of several measurements, including Mutual Information (MI), Correlation Coefficient (CC), Structural Similarity Index Metric (SSIM), Structural Content (SC), and Normalized Cross Correlation (NCC), provided a reference image was available. If the reference image was not available, the performance of the merged image would be evaluated using metrics such as Structural Blind Reference Less

Image Spatial Quality Evaluator (BRISQUE), Naturalness Image Quality Evaluator (NIQE), Perception-based Image Quality Evaluator (PIQE), and Entropy[12].

2.1.1 Quantitative analysis with a reference image

Mutual information involves quantifying information content in the source image, which was subsequently utilized to create another image. The attainment of Maximum Mutual Information is an accurate measure of the efficacy of the image fusion technique. The present concept is explained as follows:

$$MI_{AC} = \sum_{AC} P_{A,C(a,c)} \log \left[\frac{P_{AC(a,c)}}{P_{A(a)} P_{C(c)}} \right] \quad (6)$$

Where $P\_A(a)$ and $P\_C(c)$ denote the probability of the histogram of input image *A* and the fused image *C*. $P\_(A, C(a, c))$ indicates the joint histogram of input image *A* and the fused image is *C*. If mutual information value is high, it means the fusion performance is good [13].

2.1.1.1 Correlation Coefficient (CC)

Correlation Coefficient (CC) was used to compare the spectral features of a reference image (A or B) and the fused image (C). The reference and fused images are comparable when the value of CC approaches +1. Variation rises when the value of CC is lower than one [14].

$$CC = \frac{2C_C}{C_A + C_C} \quad (7)$$

CA and CC are the reference (A) and fused image (C) correlation coefficients.

2.1.1.2 Structural Similarity Index (SSIM)

It compares the local intensity structures of pixels between the source and fused images. The range is between -1 and 1. The value 1 indicates a similarity between the reference and fused images[15].

$$SSIM = \frac{(2\mu_A\mu_C + C1)(2\sigma_{AC} + C2)}{(\mu_A^2 + \mu_C^2 + C1)(\sigma_A^2 + \sigma_C^2 + C2)} \quad (8)$$

Where μ_A and μ_C are the mean intensities, σ_A and σ_C are standard deviations, σ_{AC} is the covariance of A and C, C1 and C2 are small constants for A and C, respectively.

2.1.1.3 Structural Content (SC)

A higher value of SC shows that the image has poor quality. The structural content quality metric is expressed as:

$$SC = \frac{\sum_{i=1}^{m} \sum_{j=1}^{n} \left(A_{ij}\right)^2}{\sum_{i=1}^{m} \sum_{j=1}^{n} \left(C_{ij}\right)^2} \quad (9)$$

Where *i* and *j* are the row and column numbers, m and n are the total values for row and column, and Aij and Cij are input and fuse images.

2.1.1.4 Normalized Cross Correlation (NCC)

Normalized cross-correlation is employed to determine similar content between the input and fused image[16].

$$\mathrm{NCC} = \frac{\sum_i (\mathrm{Xi} - \overline{\mathrm{X}})(\mathrm{Yi} - \overline{\mathrm{Y}})}{(\sum_i (\mathrm{Xi} - \overline{\mathrm{X}})(\mathrm{Yi} - \overline{\mathrm{Y}}))^2} \quad (10)$$

Where Xi is the input image, Yi is the fused image, x, and ¯y are the means of Xi and Yi, respectively.

2.1.2 Quantitative analysis with no reference image

This type of quality assessment can be represented as:

2.1.2.1 Blind/Referenceless Image Spatial Quality Evaluator (BRISQUE)

The proposed method employs a Support Vector Regression (SVR) model to calculate the BRISQUE measure. The model was developed in a dataset of images with corresponding Differential Mean Opinion Score (DMOS) values. The database comprised images exhibiting known distortion forms, including compression objects, blurring, and noise. Additionally, the database contained unchanged versions of the distorted images. In order to evaluate an image using the BRISQUE model, the image must contain at least one of the distortions the model was trained to recognize. This can be accomplished by utilizing the MATLAB statement [17].

2.1.2.2 Naturalness Image Quality Evaluator (NIQE)

The Naturalness Image Quality Evaluator (NIQE) calculates the input image's no-reference image quality score. It utilizes a default model created from natural scene images to compare it with the input image; a lower value returned by the NIQE function indicates that the input image has better perceptual quality [18] [19].

2.1.2.3The Perception-based Image Quality Evaluator (PIQE)

A perception-based image quality evaluator (PIQE) is a method for evaluating the quality of real-world images based on perception without requiring any reference image. It calculates the image quality score using the mean subtraction contrast normalization coefficient. Unlike other methods, PIQE is an unsupervised approach that does not rely on a learning model [20].

2.1.2.4 Entropy (En)

Entropy (En) measures the information content in a fused image. A high entropy value of a merged image indicates that it contains significant information [21].

$$En = -\sum_{g=0}^{L} h(j) \log h(j) \tag{10}$$

Where L indicates the total number of grey levels, and $h(j)$ indicates the probability density distribution of grey level j.

2.3 Algorithms

All the algorithms were programmed using MATLAB software. Firstly, a smooth-filter algorithm was designed for all fusion algorithms. The algorithm employed a window of varying sizes (3×3, 5×5, 7×7, 9×9, and 11×11) and had two directions of blur, namely from left to right and from right to left. The right-to-left blur was implemented using the code Right (:1:c2) =I (:1:c2), while the left-to-right blur was implemented using the code J Left (:c2+1:c) =I(:c2+1:c), where c2=c/2, indicated that the image column was divided by two.

The fusion algorithms were divided into two groups. The first group consisted of mathematical methods, while the second group consisted of statistical methods.

I. Mathematical methods algorithms

The mathematical fusion algorithms included addition and multiplication methods.

- In the addition methods, the resultant fused image was obtained by taking the average intensity of corresponding pixels from both input images.

Image fuse addition= I Right /2+ I Left /2.

- The Multiplication methods combined two data sets by multiplying the pixel of the first image with the pixel of the second image. Fuse equation can be written as:

*Image fuse multiplication= sqrt (I Right) *Sqrt (I Left).*

II. Statistical method algorithms

Two statistical methods were designed, each divided into two sub-methods. The first method

was standard deviation and it was divided into real and binary sub-methods, while the second method was covariance and it was divided into real and binary sub-methods.

- Real standard deviation method
  Statistical image fusion techniques come from the direct statistical techniques. This method assigns various weights to the related source images, which means that the pixels of grey value are multiplied by various factors as stated below:

  Proposed method P1= Standard deviation I Right/ (Standard deviation I Right+ Standard deviation I Left)
- Binary standard deviation method

The binary standard deviation method depends on P1 value, if it is less than 0.5, the value will be zero. If P1 value is greater than 0.5, the value is 1

- Real covariance method
  It is defined as the square of the standard deviation of a sample or a set of data and is used to analyze the factors that affect the distribution and spread of the data submitted for study. If P1 value is less than 0.5, the value will be zero.

  Proposed method P1 covariance *I Right/ (*covariance *I Right*+ covariance *I Left)*
- Binary covariance method
  The binary covariance method depends on P1 value, if it is less than 0.5, the value will be zero. If P1 value is bigger than 0.5, the value is 1

Image fused binary standard deviation = p1* I Right + (1-p1) * I Left

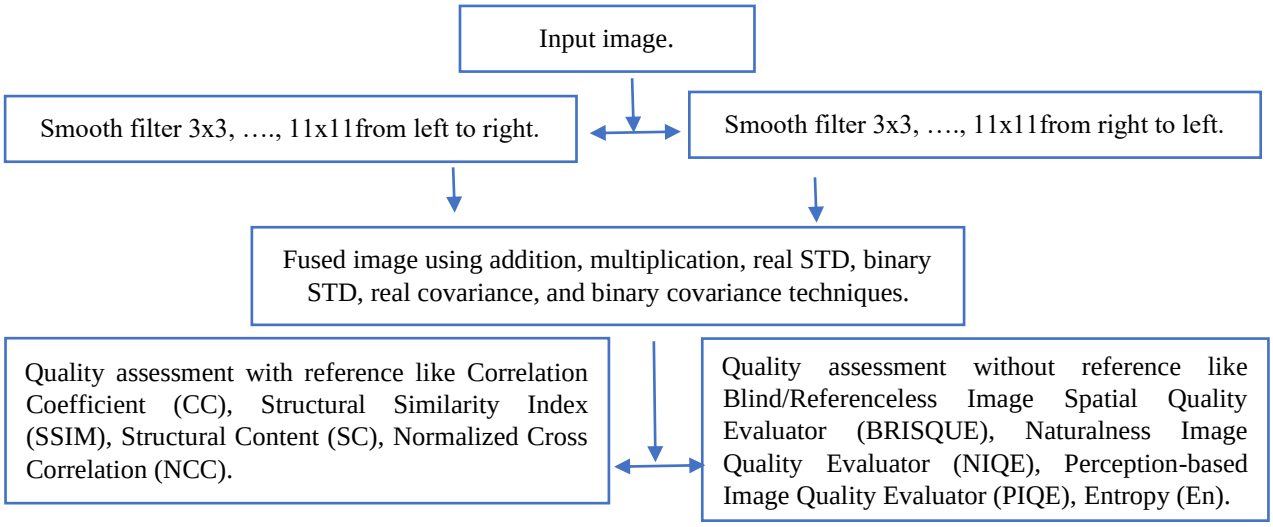

Results and Discussion

The studied images are shown in Figure (1-a) (Cameraman image) with a size of (256×256) and a bit depth of (8) bits per pixel, Figure (1-b) (Personal image) with a size of (473×467) and a bit depth of (8) bits per pixel, and Figure (1-c) (Lena image) with a size of (512×512) and a bit depth of (8) bits per pixel.

(a) **(b)** **(c)**

Figure 1: The tested images used in this study

The smooth filter method was applied to the images in Figure (1) with different sizes of windows (3× 3, 5× 5, 7× 7, 9× 9, and 11× 11). The block was shifted from left to right and from right to left, Figure (2).

(a) 3smoothfiltre right 5smoothfilter right 7smooth filter right 9smooth filter right 11smooth filter right

3 smooth filter left 5smooth filter left 7 smooth filter left 9 smooth filter left 11 smooth filter left

(b) smooth filter right 5smoothfilter right 7smooth filter right 9smooth filter right 11smooth filter right

3 smooth filter left 5smooth filter left 7 smooth filter left 9 smooth filter left 11 smooth filter left

(c) 3smoothfiltre right 5 smoothfilter right 7smooth filter right 9smooth filter right 11smooth filter right

3 smooth filter left 5 smooth filter left 7 smooth filter left 9 smooth filter left 11 smooth filter left

Figure 2: Images resulting from the process of the smooth filter towards the left and right

The resulting images of Figure (2) were fused based on six techniques (addition C Add, multiplication C Mul, real standard deviation C real-Std, binary standard deviation C Binary-Std, real covariance C real-CV and binary covariance C binary-CV), the results of the fusion techniques are shown in Figures (3), (4), and (5).

Figure 3: Cameraman fusion image using (a) Addition technique, (b) Multiplication technique, (c) Real standard deviation technique, (d) Binary standard deviation technique, (e) Real covariance technique, and (f) Binary covariance technique

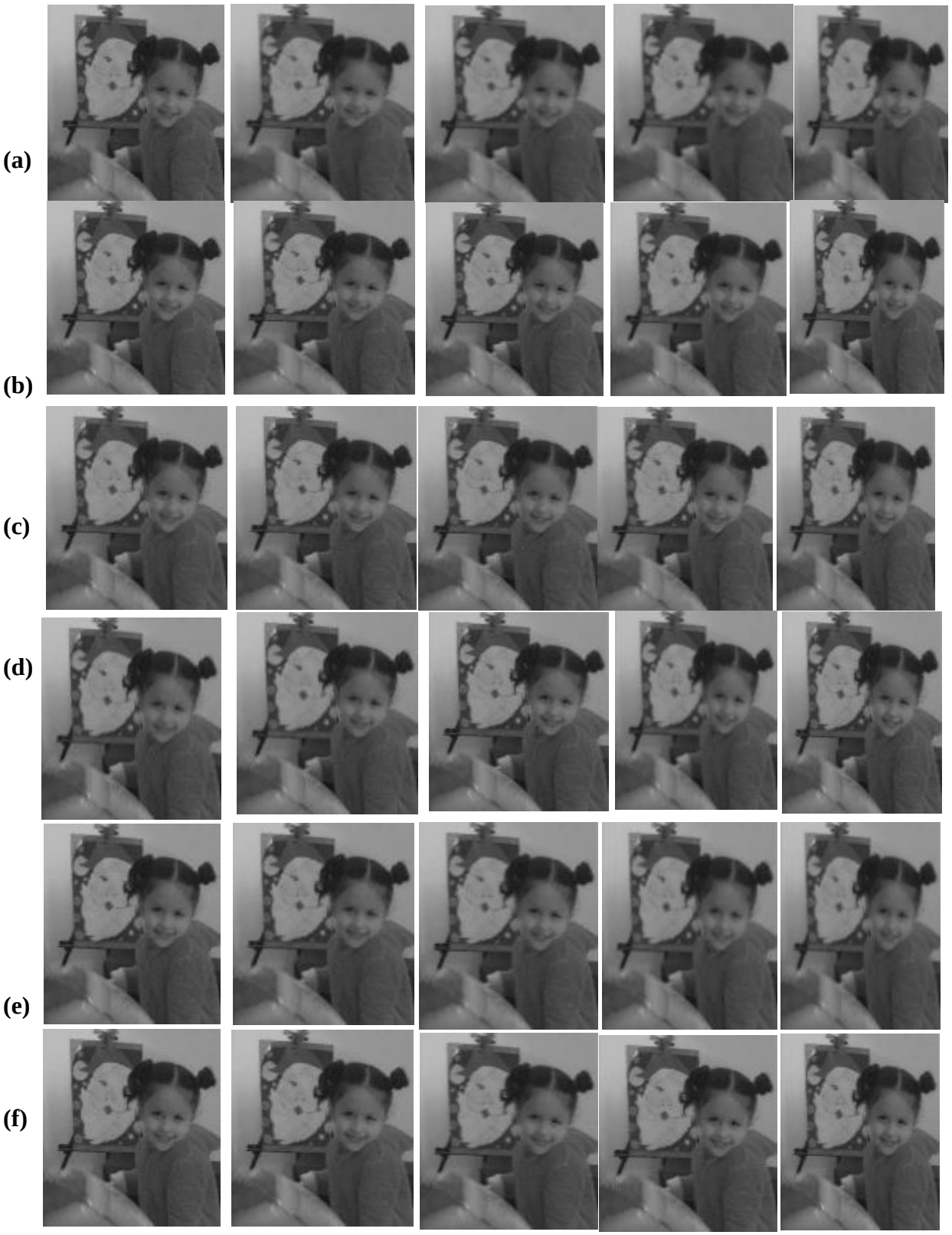

Figure 4: Personal fusion image using (a) Addition technique, (b) Multiplication technique, (c) Real standard deviation technique, (d) Binary standard deviation technique, (e) Real covariance technique, and (f) Binary covariance technique.

Figure 5: Lena fusion image using (a) Addition technique, (b) Multiplication technique, (c) Real standard deviation technique, (d) Binary standard deviation technique, (e) Real covariance technique, and (f) Binary covariance technique.

Figure (6) shows the statistical criteria concerning the smooth right image (A), smooth left image (B), and fused image (C). Figure (6i) shows the Mutual Information criteria. Figure 6i (a, c, e) shows the Mutual Information data between A and C. Figure 6i (b, d, f) shows the Mutual Information data between B and C. The three images' data in Figure (6i) are divided as Cameraman in (a, b), Lena in (c, d), and Personal in (e, f); this sequence order is the same for the remaining parts in Figure (6). Figure (6ii) shows the correlation criteria. Figure (6iii) demonstrates the Normalized cross-correlation criteria. Figure (6v) illustrates the structural

similarity index metric criteria. Figure (6iv) shows normalized criteria. Finally, Figure (6vi) illustrates structural content criteria.

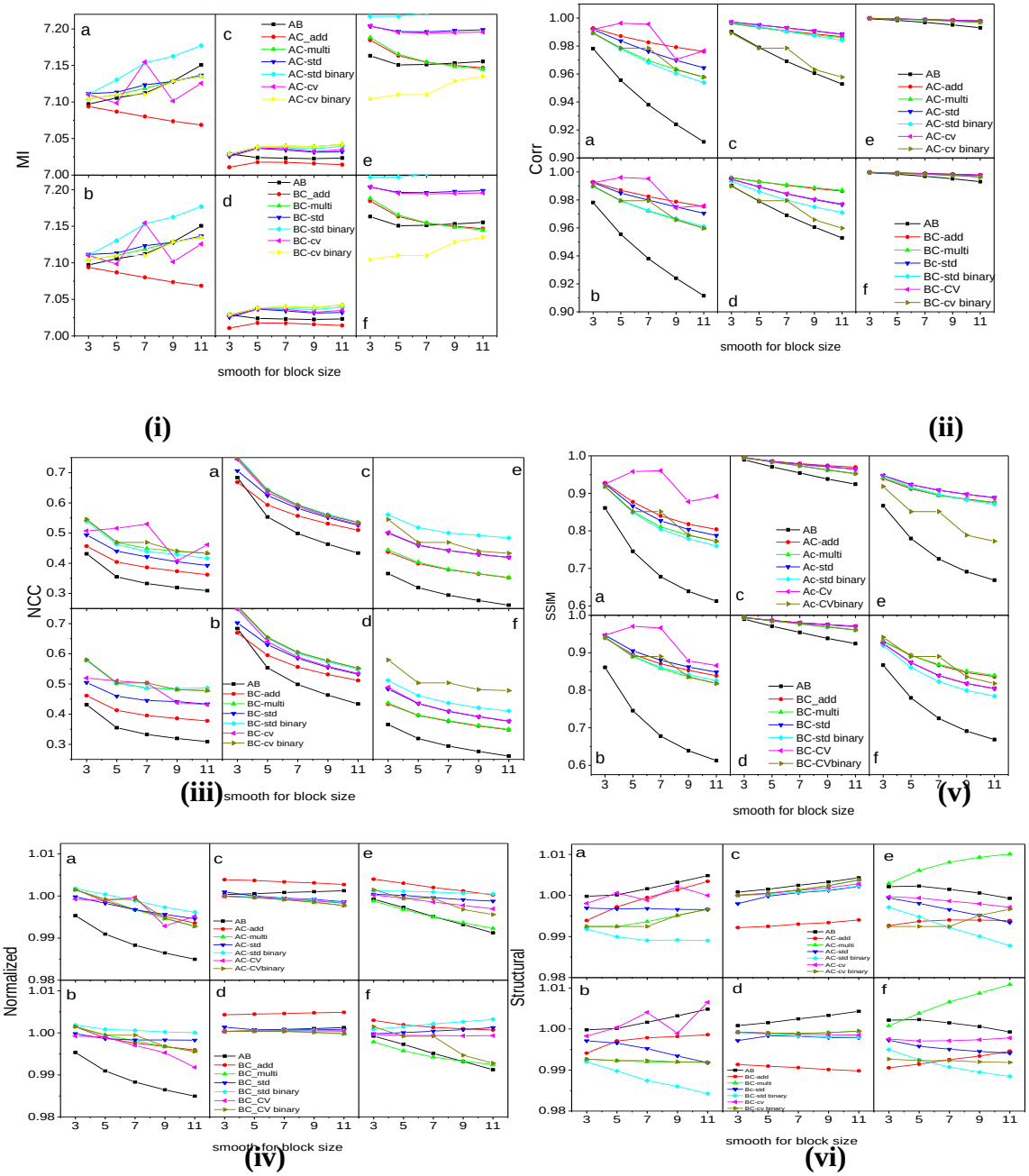

Figure 6: Quality criteria with reference for each blurred image (i) relation between Mutual Information and A, B, and C images, (ii) relation between the correlation coefficient and A, B, and C images, (iii) relation between normalized cross-correlation and A, B and C images, (v) relation between structural similarity index metric and A, B, and C images, (iv) relation between normalized A, B and C and, (vi) structural content A, B and C images.

From Figure 6, the normalized criteria show a noticeable behavior in the quality of the smooth image. Standard behavior was random with the window size; the Mutual Information and cross-correlation criteria, normalized cross-correlation criteria, and structural similarity index metric criteria show noticeable behavior of the smooth image quality. The behaver of the criteria is to increase with the increased size of the window. The higher curve of these methods is the best method. The reason behind this is mathematical equations, which depend

on pixel value or matching between the original and fused image, while structural content criteria decrease with an increased size window for all images. Evaluating the quality of the calculated fused image relied on statistical criteria without reference to sources A and B, Figures (7) for adopted images (a) cameraman, (b) Lena, and (c) personal image. The data explain the relation between A, B, and C criteria.

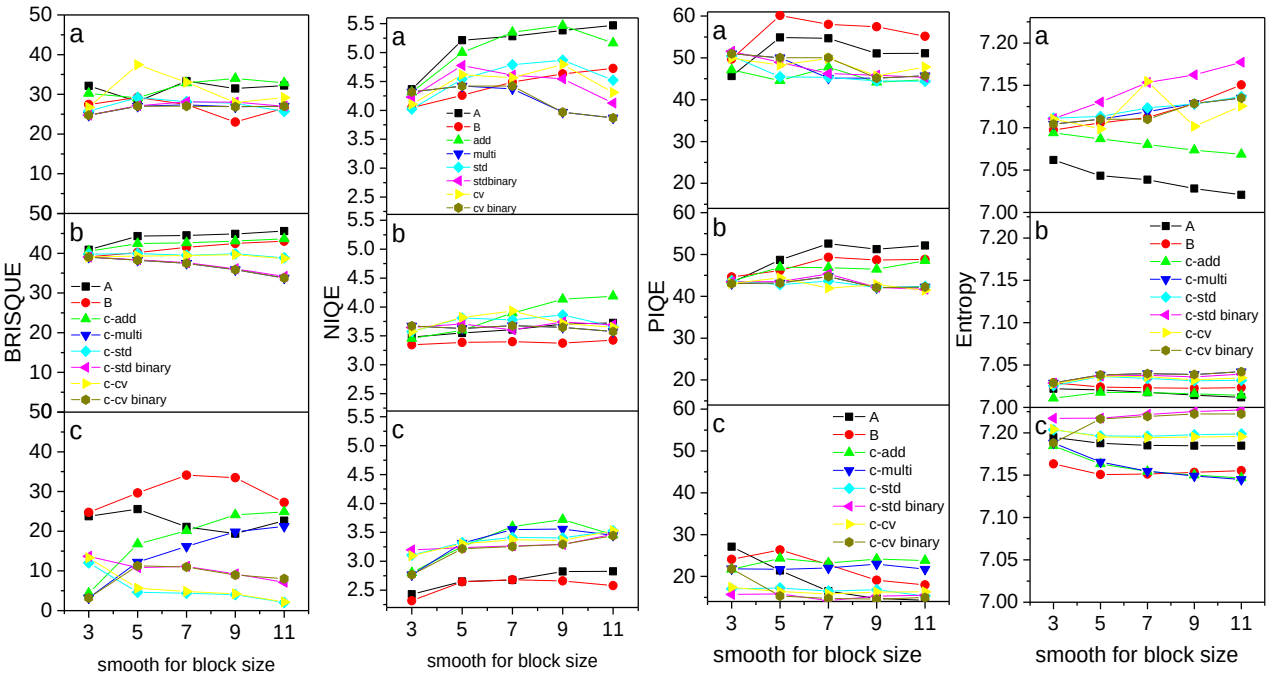

Figure 7: Quality criteria without reference for each blurred image, (i) BRISQUE for A, B, and C images, (ii) NIQE for A, B, and C images, (iii) PIQE for A, B, and C images, (v) Entropy for A, B and C images.

Figure 7 shows that the behavior of brisque was random with increasing window size, while NIQE entropy was increasing behavior with increasing window size, and PIQE behavior was decreasing with increasing window size.

Conclusion

The smoothed image was simulated using a smooth filter (half left and half right) with size windows of (3×3), (5×5), (7×7), (9×9), and (11×11) pixels. The image resulting from the smooth filter towards the right was combined with the image from the smooth filter towards the left using traditional techniques such as addition, multiplication, and new suggested techniques, namely absolute real standard deviation, binary standard deviation, real covariance, and binary covariance. The performance of these methods was evaluated using 10 types of criteria (six with reference and four without reference). Lena's image showed a different behavior than that of the cameraman and the personal because Lena's image had more details, resolution, and sharper contrasts. The best combination method was binary standard division, depending on the quality standards. The correlation behavior in Figure 6 (a), the reference image (AB), had a value of 0.98 and decreased with the increase of the filter mask to reach 0.91. At the same time, the fusion image-like additive had a value of 0.99 and decreased to reach 0.98 with an increase of filter mask, respectively.

References

[1] J. Du, W. Li, K. Lu, and B. Xiao, "An overview of multi-modal medical image fusion," *Neurocomputing*, vol. 215, pp. 3-20, 2016.

[2] F. I. Abbas, N. M. Mirza, A. H. Abbas, and L. H. Abbas, "Enhancement of wheat leaf images using fuzzy-logic based histogram equalization to recognize diseases," *Iraqi Journal of Science*, pp. 2408-2417, 2020.

[3] Z. Hou, K. Lv, X. Gong, and Y. Wan, "A Remote Sensing Image Fusion Method Combining Low-Level Visual Features and Parameter-Adaptive Dual-Channel Pulse-Coupled Neural Network," *Remote Sensing*, vol. 15, no. 2, p. 344, 2023.

[4] H. K. Abbas, A. H. Al-Saleh, H. J. Mohamad, and A. A. Al-Zuky, "New algorithms to enhanced fused images from auto-focus images," *Baghdad Sci. J*, vol. 10, no. 18, p. 1, 2021.

[5] D. Rao, X.-J. Wu, and T. Xu, "Tgfuse: An infrared and visible image fusion approach based on transformer and generative adversarial network," *arXiv preprint arXiv:2201.10147*, 2022.

[6] X. Jin, X. Xi, D. Zhou, X. Ren, J. Yang, and Q. Jiang, "An unsupervised multi-focus image fusion method based on Transformer and U-Net," *IET Image Processing*, vol. 17, no. 3, pp. 733-746, 2023.

[7] M. A. Mohammed, A. J. Hatem "Change detection of the land cover for three decades using remote sensing data and geographic information system" *AIP Conference Proceedings 2307, 020029 (2020); https://doi.org/10.1063/5.0033261*.

[8] D. N. H. Thanh and S. Engínoğlu, "An iterative mean filter for image denoising," *IEEE Access*, vol. 7, pp. 167847-167859, 2019.

[9] W. Zhou *et al.*, "Improved estimation of motion blur parameters for restoration from a single image," *Plos one*, vol. 15, no. 9, p. e0238259, 2020.

[10] N. H. Resham, H. K. Abbas, H. J. Mohamad, and A. H. Al-Saleh, "Noise Reduction, Enhancement and Classification for Sonar Images," *Iraqi Journal of Science*, pp. 4439-4452, 2021.

[11] H. K. Abbas, A. H. Al-Saleh, and A. A. Al-Zuky, "Optical Images Fusion Based on Linear Interpolation Methods," *Iraqi Journal of Science*, vol. 60, no. 4, pp. 924-936, 2019.

[12] G.-H. Gwon, J. H. Lee, I.-H. Kim, and H.-J. Jung, "CNN-based Image Quality Classification Considering Quality Degradation in Bridge Inspection using an Unmanned Aerial Vehicle," *IEEE Access*, 2023.

[13] M. Zhou, K. Yan, J. Huang, Z. Yang, X. Fu, and F. Zhao, "Mutual information-driven pan-sharpening," in *Proceedings of the IEEE/CVF Conference on Computer Vision and Pattern Recognition*, 2022, pp. 1798-1808.

[14] W. Lu *et al.*, "Blind Surveillance Image Quality Assessment via Deep Neural Network Combined with the Visual Saliency," in *Artificial Intelligence: Second CAAI International Conference, CICAI 2022, Beijing, China, August 27–28, 2022, Revised Selected Papers, Part II*, 2023: Springer, pp. 136-146.

[15] Q. Sang, Y. Yang, L. Liu, X. Song, and X. Wu, "Image quality assessment based on quaternion singular value decomposition," *IEEE Access*, vol. 8, pp. 75925-75935, 2020.

[16] L. Wu and L. Zhao, "ISAR Image Registration Based on Normalized Correlation Coefficient," in *2023 IEEE 3rd International Conference on Power, Electronics and Computer Applications (ICPECA)*, 2023: IEEE, pp. 354-359.

[17] B. K. Shah, V. Kedia, R. Raut, S. Ansari, and A. Shroff, "Evaluation and comparative study of edge detection techniques," *IOSR Journal of Computer Engineering*, vol. 22, no. 5, pp. 6-15, 2020.

[18] L. Wu, X. Zhang, H. Chen, D. Wang, and J. Deng, "VP-NIQE: An opinion-unaware visual perception natural image quality evaluator," Neurocomputing, vol. 463, pp. 17-28, 2021.

[19] H. K. Abbas Al-Aarajy, A. A. Zaeen, and K. I. Abood, "Supervised Classification Accuracy Assessment Using Remote Sensing and Geographic Information System," TEM Journal, vol. 13, no. 1, 2024.

[20] W. Kim and C. Yim, "No-reference Image Contrast Quality Assessment based on the Degree of Uniformity in Probability Distribution," IEEE Transactions on Smart Processing & Computing, vol. 11, no. 2, pp. 85-91, 2022.

[21] S. K. Panguluri and L. Mohan, "Discrete wavelet transform based image fusion using unsharp masking," *Periodica Polytechnica Electrical Engineering and Computer Science*, vol. 64, no. 2, pp. 211-220, 2020.